Wireless Personal Communications (2022) 122:2621–2637
https://doi.org/10.1007/s11277-021-09021-x

Non Orthogonal Multiple Access for Millimeter Wave Communications Using Intelligent Reflecting Surfaces

Raed Alhamad[1] · **Hatem Boujemaa**[2]

Accepted: 16 August 2021 / Published online: 26 August 2021

Abstract

In this paper, we suggest the use of Intelligent Reflecting Surfaces (IRS) for Non Orthogonal Multiple Access (NOMA) using millimeter wave communications. The source sends a combination of K symbols dedicated to K users. The received signal at relay node R is affected with P interferers. The relay node detects the symbol of the weak user as it is transmitted with the largest power. Then, it uses Successive Interference Cancelation (SIC) to remove the contribution of the signal of the weak user to detect the symbol of the second weakest user. The rest of the detections are performed similarly until relay node detects all K symbols. The relay node sends a combination of the detected symbols. The transmitted signal by the relay node is reflected by different sets of IRS reflectors. The reflected signals reach the i-th user with the same phase. The phase shift of i-th IRS reflector depends on the phase of channel coefficient between relay and IRS as well as the phase of channel coefficient between IRS and user. The i-th strong user uses SIC to detect the symbols of $K-i-1$ weak users to be able to detect its symbol. We optimize the fraction of powers allocated to NOMA users at the source and relay node to maximize the total throughput. The results are valid for Nakagami channels and any number of interferers at the relay and NOMA users. When there are two users, a total throughput of 3.5 bit/s/Hz is reached for 16QAM modulation and average SNR per bit equal to −22.7 dB, −19.7 dB, −16.6 dB, −13.6 dB, −10.4 dB, −7.2 dB, −3.8 dB and 6.5 dB respectively for a number of reflectors per user $N = 512, 256, 128, 64, 32, 16, 8$ and when there is no IRS. For $N = 32$ reflectors, optimal power allocation allows 2.1 dB gain with respect to fixed power allocation. When there are three users, a total throughput of 2.5 bit/s/Hz is reached for QPSK modulation and average SNR per bit equal to −10.7 dB, −7.6 dB, −4.3 dB and 6.9 dB for a number of reflectors per user $N = 32, 16, 8$ and when there is no IRS.

Keywords IRS · RF · Millimeter wave communications · Nakagami channels

✉ Raed Alhamad
ralhamad@seu.edu.sa

Hatem Boujemaa
boujemaa.hatem@supcom.tn

[1] Information Technology Department, Saudi Electronic University, Riyadh, Kingdom of Saudi Arabia

[2] COSIM-SUP'COM, Tunis, Tunisia

1 Introduction

Millimeter wave communications (mmwave) offer data rates of the order of 10 Gb/s since the used bandwidth is going from 30 to 300 GHZ [1–4]. Millimeter wave signals cannot penetrate through walls and building and relaying techniques are mandatory [1–7]. Multihop relaying can be used when the source is far from the destination [6–12]. When multiple branches are available, we can activate the branch with the highest end-to-end Signal to Interference plus Noise Ratio (SINR). Both Amplify and Forward (AF) and Decode and Forward (DF) relaying can be used [8]. AF relays amplify the received signal and forward it to the next relay. AF relaying uses a constant amplification gain and these are known as blind relays. Otherwise, non-blind relays use an adaptive amplification factor that depends on the channel coefficient. DF relays decode and regenerate the transmitted signal [9, 10]. In DF relaying, the relay node transmits only if it has correctly detected the received packet. The use of relay nodes is complex to implement since relay selection techniques require many signalization. Besides, the throughput is low if all relays transmit without relay selection since multiple orthogonal channels are required.

Intelligent Reflecting Surfaces (IRS) have been suggested to enhance the throughput of wireless communications [11–15]. The transmitted signal by the source is reflected by IRS reflectors and reaches the destination with a null phase. The phase shift of i-th reflector depends on the phase of channel coefficient between the source and i-th IRS reflector as well as the phase of channel coefficient between i-th reflector and destination [16–18]. Different sets of reflectors are dedicated to different NOMA users [19]. The reflected signals over each set of reflectors reach the corresponding user with a null phase [19]. IRS have been recently suggested for mmwave communications [20, 21]. However, the derived results in [20, 21] correspond to Orthogonal Multiple Access (OMA) that offers lower data rates than NOMA. Exact and asymptotic performance analysis of wireless communications using IRS were derived in [22–24]. Some experimental results of wireless networks using IRS have been discussed in [25].

Millimeter wave communications using multiple antennas for NOMA systems were proposed in [26, 27]. Relaying techniques for millimeter wave communications using NOMA were studied in [28]. The coverage of millimeter wave communications using NOMA was studied in [29]. Precoding and combining techniques for millimeter wave communications were suggested in [30]. Deep learning for millimeter wave communications was suggested in [31]. A high gain antenna was used in [32] to improve the throughput of millimeter wave communications.

To the best of our knowledge, mmwave communications using NOMA and IRS have not been yet suggested and analyzed in [1–32]. The contributions of the paper are;

- We suggest the use of Intelligent Reflecting Surfaces (IRS) for NOMA systems using millimeter wave communications. The source sends a combination of K symbols dedicated to K users. The received signal by the relay node is affected by P interferers. The relay node uses SIC to detect the symbols of K users. Then, it sends a combination of detected symbols. The transmitted signal by the relay node is reflected by different sets of IRS reflectors dedicated to different users. We show that the reflected signals have the same phase at each NOMA user.
- The proposed NOMA using IRS offers 10, 13, 16, 20, 24, 27 and 30 dB gain with respect to conventional NOMA using millimeter wave communications without IRS

for a number of reflectors $N = 8, 16, 32, 64, 128, 256, 512$. Besides, mmwave using NOMA offers larger data rates than OMA as suggested in [20, 21].

- We also suggest optimizing the powers allocated to NOMA users at the source and relay node to enhance the total throughput. The paper contains six sections. Next section studies the performance of millimeter wave link in the presence of P interferers at the relay node. Section 3 evaluates the outage probability at any user using intelligent reflecting surfaces. Section 4 optimizes the total throughput by adjusting the fraction of powers dedicated to K NOMA users. Section 5 gives some theoretical and simulation results. Section 6 concludes the paper.

2 Millimeter Wave Link

The system model provided in Fig. 1 contains a source S, a relay node R and K users U_i, $i = 1, \dots K$. U_i is the i-th strong user. We assume Nakagami channel between all nodes and we denote by M the m-fading figure. The source sends a combination of K symbols s_i, $i = 1, 2, \dots K$ dedicated to K users:

$$s = \sqrt{E_S} \sum_{i=1}^{K} \sqrt{C_i} s_i \tag{1}$$

where E_S is the Transmitted Energy per Symbol (TES) of the source, $0 < C_i < 1$ is the fraction of power allocated to user U_i. Less power is allocated to the strong user: $0 < C_1 < C_2 < \dots < C_K$. We have

$$\sum_{i=1}^{K} C_i = 1. \tag{2}$$

We assume that the received signal at R is affected by P interferers: [1–5]

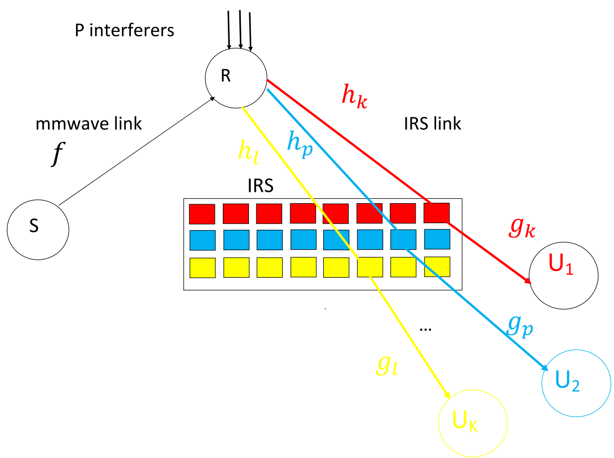

Fig. 1 Millimeter wave communications using IRS

$$r = fs + I = f\left[\sqrt{E_s}\sum_{i=1}^{K}\sqrt{C_i}s_i\right] + I. \tag{3}$$

where f is the channel coefficient between S and R, I is the interference term at R composed of P interferers:

$$I = \sum_{q=1}^{P} E_q|i_q|^2 \tag{4}$$

E_q is the TES of q-th interferer, i_q is the channel coefficient between q-th interferer and R.

The relay node detects the symbol of user U_K since it is received with the largest power. The SINR is equal to

$$\Gamma_{R,K} = \frac{C_K E_S|f|^2}{I + E_S|f|^2\sum_{i=1}^{K-1}C_i} \tag{5}$$

Then, relay R removes the contribution of s_K using SIC to detect s_{K-1} with SINR

$$\Gamma_{R,K-1} = \frac{C_{K-1}E_S|f|^2}{I + E_S|f|^2\sum_{i=1}^{K-2}C_i} \tag{6}$$

The remaining detections are made similarly, R will detect s_p $p = K, K-1, \dots, 1$ with SINR

$$\Gamma_{R,p} = \frac{C_p E_S|f|^2}{I + E_S|f|^2\sum_{i=1}^{p-1}C_i} \tag{7}$$

The Cumulative Distribution Function (CDF) of $\Gamma_{R,p}$ is equal to

$$\begin{aligned} F_{\Gamma_{R,p}}(x) &= P\left(\frac{C_p E_S|f|^2}{I + E_S|f|^2\sum_{i=1}^{p-1}C_i} \le x\right) = P\left(\frac{C_p U}{1 + U\sum_{i=1}^{p-1}C_i} \le x\right) \\ &= F_U\left(\frac{x}{C_p - x\sum_{i=1}^{p-1}C_i}\right) \end{aligned} \tag{8}$$

where $F_U(x)$ is the CDF of U where

$$U = \frac{E_S|f|^2}{I} \tag{9}$$

There is no outage at R if all SINR $\Gamma_{R,1}, \Gamma_{R,2}, \dots, \Gamma_{R,K}$ are larger than x:

$$\begin{aligned} P_{outage,R}(x) &= 1 - P(\Gamma_{R,1} > x, \dots, \Gamma_{R,K} > x) \\ &= F_U\left(\max_{1\le p\le K}\left(\frac{x}{C_p - x\sum_{i=1}^{p-1}C_i}\right)\right) \end{aligned} \tag{10}$$

For Nakagami fading channels, $X = E_S|f|^2$ follows a Gamma distribution $Gamma(M, \beta)$ defined as

$$f_X(x) = \frac{x^M e^{-\frac{x}{\beta}}}{\Gamma(M)\beta^M} \tag{11}$$

$M > 0.5$ is the m-fading figure of Nakagami channel,

$$\beta = \frac{E_S E(|f|^2)}{M} \tag{12}$$

$E(.)$ is the expectation operator.

The interference I at the relay node is expressed as

$$I = \sum_{q=1}^{P} I_q \tag{13}$$

where $I_q = E_q|i_q|^2$

I_q has a Gamma distribution $Gamma(M, \alpha)$

$$\alpha = \frac{E(I_q)}{M} \tag{14}$$

The sum of P independent Gamma random variables (r.v.) I_q is a Gamma r.v. $Gamma(PM, \alpha)$. We deduce that $U = \frac{X}{I}$ is the quotient of two Gamma r.v. that has a general prime distribution and Probability Density Function (PDF) [33]:

$$f_U(x) = \frac{\Gamma(M+PM)\alpha^M x^{M-1}(1+\frac{x\alpha}{\beta})^{-PM-M}}{\beta^M\Gamma(M)\Gamma(PM)} \tag{15}$$

The proof is provided in "Appendix A".

We have [34]

$$_2F_1(a,\, b; c; z) = \frac{\Gamma(c)}{\Gamma(b)\Gamma(c-b)} \times \int_0^1 x^{b-1}(1-x)^{c-b-1}(1-zx)^{-a}dx \tag{16}$$

where $_2F_1(a,b;c;z)$ is the hypergeometric function. We use (16) to write the CDF of SINR as

$$F_U(x) ={}_2F_1\left(PM+M, M; M+1, \frac{-x\alpha}{\beta}\right) \times \frac{\Gamma(M+PM)(x\alpha)^M}{\Gamma(M)\Gamma(PM)\beta^M} \tag{17}$$

When there is Additive White Gaussian Noise (AWGN), the SINR can be upper bound by

$$\Gamma_{R,p,AWGN} = \frac{C_p E_S|f|^2}{N_0 + I + E_S|f|^2\sum_{i=1}^{p-1} C_i} < \Gamma_{R,p} = \frac{C_p E_S|f|^2}{I + E_S|f|^2\sum_{i=1}^{p-1} C_i} \tag{18}$$

The derived outage probability in (10) is a lower bound.

When there is AWGN, we can derive numerically the outage probability. In fact, we can write

$$\Gamma_{R,p,AWGN} = \frac{C_p E_S|f|^2}{N_0 + I + E_S|f|^2\sum_{i=1}^{p-1} C_i} = \frac{C_p X}{N_0 + I + X\sum_{i=1}^{p-1} C_i} \tag{19}$$

The CDF of $\Gamma_{R,p,AWGN}$ can be computed numerically as

$$F_{\Gamma_{R,p,AWGN}}(x) = \int_0^{+\infty} F_X\left(\frac{x(N_0+y)}{C_p - x\sum_{i=1}^{p-1} C_i}\right) f_I(y)dy \tag{20}$$

$F_X(z)$ is the CDF of X given by

$$F_X(x) = \frac{\gamma\left(M, \frac{x}{\beta}\right)}{\Gamma(M)} \tag{21}$$

$\Gamma(M)$ is the Gamma function and

$$\gamma(M,x) = \int_0^x t^{M-1}e^{-t}dt, \tag{22}$$

and $f_I(y)$ is the PDF of I given by

$$f_I(y) = \frac{y^{PM-1}e^{-\frac{y}{\alpha}}}{\Gamma(MP)\alpha^{MP}} \tag{23}$$

Therefore, in the presence of AWGN, the outage probability at R is similarly as

$$P_{outage,R,AWGN}(x) = \int_0^{+\infty} F_X\left(\max_{1\leq p\leq K}\left(\frac{x(N_0+y)}{C_p - x\sum_{i=1}^{p-1} C_i}\right)\right) f_I(y)dy \tag{24}$$

3 IRS Link

To extend the coverage of millimeter wave communications and to serve K NOMA users, IRS is placed between relay node R and users $U_1, U_2, \dots, U_K$. We define h_k as the channel coefficient between R and k-th IRS reflector with average power $E(|h_k|^2) = \frac{1}{d^{ple}}$ where $E(.)$ is the expectation operator, ple is the path loss exponent and d is the distance between R and IRS. We define $g_k \in I_i$ as the channel coefficient between k-th reflector of IRS and user U_i with average power $E(|g_k|^2) = \frac{1}{d_i^{ple}}$ where d_i is the distance between IRS and U_i. I_i is the set of IRS reflectors dedicated to user U_i.

Let a_k and b_k be the absolute value and phase of $h_k = a_k e^{-jb_k}$. For Nakagami channels, a_k has a Gamma distribution with $E(a_k) = \frac{\Gamma(M+0.5)}{\Gamma(M)}\sqrt{\frac{1}{Md_1^{ple}}}$ and $E\left(a_k^2\right) = E(|h_k|^2) = \frac{1}{d^{ple}}$ [36]. Let c_k and d_k be the absolute and phase of $g_k = c_k e^{-jd_k}$. We have $E(c_k) = \frac{\Gamma(M+0.5)}{\Gamma(M)}\sqrt{\frac{1}{Md_i^{ple}}}$ and $E\left(c_k^2\right) = E(|g_k|^2) = \frac{1}{d_i^{ple}}$ [36].

IRS optimizes the phase ϕ_k of k-th reflector as follows

$$\phi_k = b_k + d_k. \tag{25}$$

The received signal at U_i is equal to

$$r = S\sqrt{E_R}\sum_{q\in I_i} h_q g_q e^{j\phi_q} + n \tag{26}$$

where I_i is the set of reflectors dedicated to U_i, S is the transmitted NOMA symbol by relay node R, n is zero-mean Gaussian r.v. with variance N_0 and E_R is the TES of R.

Let $\hat{s}_i$ the i-th detected symbol at relay node R. When the detection is successful at the relay $\hat{s}_i = s_i$. The transmitted NOMA symbol S by relay R is written as

$$S = \sum_{l=1}^{K} \sqrt{D_l}\hat{s}_l \tag{27}$$

D_l is the fraction of power dedicated at U_l at relay R. Less power is dedicated to strong user: $0 < D_1 < D_2 < \cdots < D_K$. The sum of fraction of powers dedicated to of all users is one: $\sum_{l=1}^{K} D_l = 1$.

Using (26) and (27), we have

$$r = \sqrt{E_R}\left[\sum_{l=1}^{K} \sqrt{D_l}\hat{s}_l\right]\sum_{q\in I_i} h_q g_q e^{j\phi_q} + n \tag{28}$$

Using (25) and (28), we obtain

$$r = \sqrt{E_R}A_i\left[\sum_{l=1}^{K} \sqrt{D_l}\hat{s}_l\right] + n, \tag{29}$$

where

$$A_i = \sum_{q\in I_i} a_q c_q. \tag{30}$$

Using the Central Limit Theorem (CLT), A_i can be approximated by a Gaussian r.v. with mean $m_{A_i} = \frac{N_i\Gamma(M+0.5)^2}{M\Gamma(M)^2 d^{ple/2} d_i^{ple/2}}$ and variance $\sigma_{A_i}^2 = \frac{N_i}{d_i^{ple} d^{ple}}\left[1 - \frac{\Gamma(M+0.5)^4}{M^2\Gamma(M)^4}\right]$, $N_i = |I_i|$ is the number of IRS reflectors dedicated to U_i,.

The CDF of A_i^2 is written as

$$\begin{aligned} F_{A_i^2}(x) &= P\left(A_i^2 \le x\right) = P(-\sqrt{x} \le A_i \le \sqrt{x}) \\ &\simeq 0.5erfc\left(\frac{-\sqrt{x} - m_{A_i}}{\sqrt{2}\sigma_{A_i}}\right) - 0.5erfc\left(\frac{\sqrt{x} - m_{A_i}}{\sqrt{2}\sigma_{A_i}}\right) \end{aligned} \tag{31}$$

User U_i detects first the symbol of user U_K as $D_K > D_i\ \forall i \neq K$. The corresponding SINR is expressed as

$$\Gamma_{U_i,K} = \frac{E_R A_i^2 D_K}{N_0 + E_R A_i^2 \sum_{l=1}^{K-1} D_l} \tag{32}$$

User U_i removes the signal of U_K using SIC and detect the symbol of U_{K-1} with SINR

$$\Gamma_{U_i,K-1} = \frac{E_R A_i^2 D_{K-1}}{N_0 + E_R A_i^2 \sum_{l=1}^{K-2} D_l} \tag{33}$$

User U_i detects the symbols of users U_p $p = K, K-1, \dots, i$ with SINR

$$\Gamma_{U_i,p} = \frac{E_R A_i^2 D_p}{N_0 + E_R A_i^2 \sum_{l=1}^{p-1} D_l} \tag{34}$$

There is no outage at U_i when all SINRs are larger than x:

$$\begin{aligned} P_{outage,U_i}(x) &= 1 - P(\Gamma_{U_i,K} > x, \Gamma_{U_i,K-1} > x, \dots, \Gamma_{U_i,i} > x) \\ &= F_{A_i^2}\left(\max_{i \le p \le K}\left(\frac{N_0 x}{E_R D_p - x E_R \sum_{l=1}^{p-1} D_l}\right)\right) \end{aligned} \tag{35}$$

3.1 IRS Link Analysis in the Presence of P_i Interferers at User U_i

Figure 2 depict the system model in the presence of P_i interferers user U_i. User U_i detects the symbols of users U_p $p = K, K-1, \dots, i$ with SINR

$$\Gamma_{U_i,p} = \frac{E_R A_i^2 D_p}{N_0 + J_i + E_R A_i^2 \sum_{l=1}^{p-1} D_l} \tag{36}$$

where J_i is the interference at U_i expressed as

$$J_i = \sum_{q=1}^{P_i} J_{i,q} \tag{37}$$

$J_q = E_q' |j_q|^2$, E_q' is the TES of q-th interferer and j_q is the channel coefficient between q-th interferer and D. J_q are assumed to be i.i.d so that the J_i follows a Gamma distribution $Gamma(P_i M, \zeta_i)$ written as

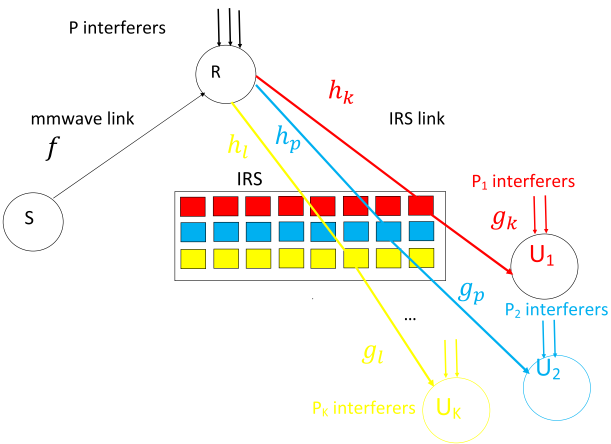

Fig. 2 Millimeter wave communications using IRS in the presence of P_i interferers at user U_i

$$f_{J_i}(y) = \frac{y^{P_iM-1}e^{-\frac{y}{\zeta_i}}}{\Gamma(MP_i)\zeta_i^{MP_i}} \tag{38}$$

where $\zeta_i = \frac{E(J_{i,q})}{M}$.

In the presence of P_i interferers at U_i, the outage probability at U_i is computed numerically as follows

$$P_{outage,U_i}(x) = \int_0^{+\infty} F_{A_i^2}\left(\max_{i\leq p\leq K}\left(\frac{(N_0+y)x}{E_RD_p - xE_R\sum_{l=1}^{p-1}D_l}\right)\right)f_{J_i}(y)dy, \tag{39}$$

where $f_{J_i}(y)$ is the PDF of interference at U_i (38) and $F_{A_i^2}(x)$ is provided in (31).

4 Throughput Optimization

The end-to-end (e2e) outage probability at user U_i is computed as

$$P_{outage,e2e,U_i}(x) = 1 - \left[1 - P_{outage,U_i}(x)\right]\left[1 - P_{outage,R}(x)\right]. \tag{40}$$

There is no outage at user U_i if there is no outage event in the first hop at R and in the second hop.

An upper bound of Packet Error Probability (PEP) is expressed as [35]

$$PEP_i\left(D_1, D_2, \dots, D_K, C_1, C_2, \dots, C_K\right) < P_{outage,e2e,U_i}(W_O) \tag{41}$$

where W_0 is a waterfall threshold evaluated as [35]

$$W_0 = \int_0^{+\infty} 1 - \left[1 - 2\left(1 - \frac{1}{\sqrt{Q}}\right)erfc\left(\sqrt{\frac{3y}{Q-1}}\right)\right]^L dy \tag{42}$$

and L is packet length in Quadrature Amplitude Modulation (QAM) symbols, Q is the constellation size.

We deduce the throughput at user U_i:

$$Thr_i(D_1, D_2, \dots, D_K, C_1, C_2, \dots, C_K) = 0.5\log_2(Q)[1 - PEP_i(D_1, D_2, \dots, D_K, C_1, C_2, \dots, C_K)] \tag{43}$$

The total throughput is given by

$$Thr(D_1, D_2, \dots, D_K, C_1, C_2, \dots, C_K) = \sum_{i=1}^{K} Thr_i(D_1, D_2, \dots, D_K, C_1, C_2, \dots, C_K) \tag{44}$$

We optimize the fraction of powers allocated to users at the source (C_i) and relay (D_i) to enhance the total throughput

$$Thr^{\max} = \max_{0<D_1<D_2<\cdots<D_K<1, 0<C_1<C_2<\cdots<C_K<1} Thr(D_1, D_2, \dots, D_K, C_1, C_2, \dots, C_K) \tag{45}$$

under constraints $\sum_{i=1}^{K} C_i = 1$ and $\sum_{i=1}^{K} D_i = 1$.

5 Theoretical and Simulation Results

This section provides some theoretical and simulation results when there are $K = 2$ and $K = 3$ NOMA users and $ple = 3$. The distance between S and R is 1.5 and the distance between R and IRS is $d = 2$. The distance between IRS and users are $d_1 = 1$, $d_2 = 1.5$ and $d_3 = 2$. The number of interferers at R is $P = 3$. The number of interferers at users is $P_1 = 2$, $P_2 = 3$ and $P_3 = 4$. The m-fading figure is $M = 2$. The same powers were allocated to S and R, i.e. $E_S = E_R = E_s/2$ where E_s is the TES.

Figures 3 and 4 depict the throughput at weak and strong users for $K = 2$ and 16QAM modulation. The fraction of powers allocated to users are $C_1 = 0.4 = 1 - C_2$ and $D_1 = 0.4 = 1 - D_2$. The number of reflectors per user is $N = N_1 = N_2 = 8, 16, 32$. The proposed NOMA system using IRS offers 10, 13, 16 dB gain with respect to conventional NOMA using millimeter wave communications without IRS.

Figure 5 depicts the total throughput for 16QAM modulation. For fixed power allocation given by $C_1 = 0.4 = 1 - C_2$ and $D_1 = 0.4 = 1 - D_2$, the proposed NOMA system using IRS offers 10, 13, 16 dB gain with respect to conventional NOMA using millimeter wave communications. For an Optimal Power Allocation (OPA) maximizing the total throughput (45), the proposed NOMA using IRS offers 19 dB gain for a number of reflectors per user $N = N_1 = N_2 = 32$.

Figure 6 depicts the total throughput when there are two NOMA users for 16QAM modulation. Figure 6 shows the total throughput for a large number of reflectors $N = N_1 = N_2 = 64, 128, 256, 512$. The proposed NOMA system using IRS offers 20, 24, 27 and 30 dB gain with respect to conventional NOMA using millimeter wave communications for $N = N_1 = N_2 = 64, 128, 256, 512$.

The required E_b/N_0 in dB to reach a total throughput of 3.5 bit/s/Hz is provided in Table 1 for different values of N. We used the results of Figs. 5 and 6 with two NOMA users and 16QAM modulation.

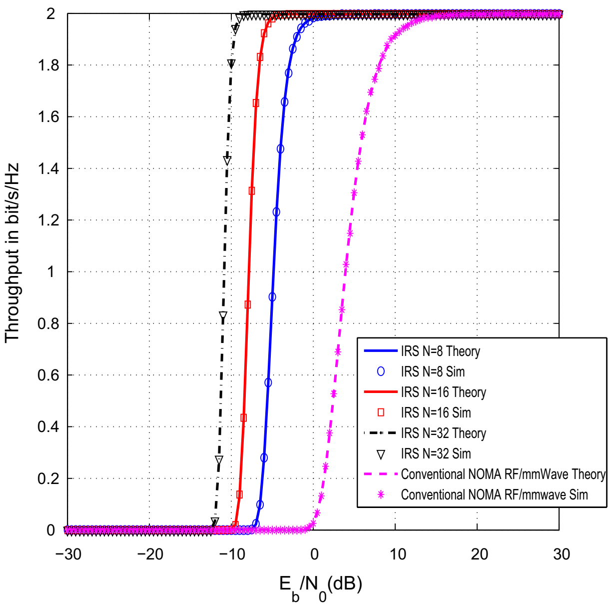

Fig. 3 Throughput at weak user for 16QAM modulation: 2 users

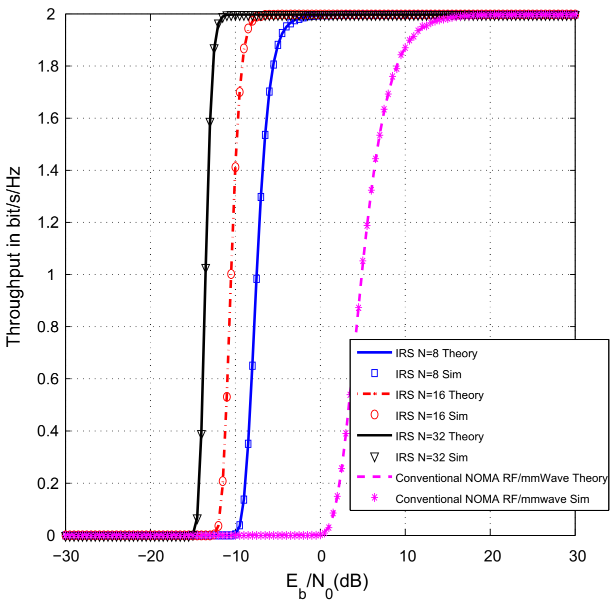

Fig. 4 Throughput at strong user for 16QAM modulation: 2 users

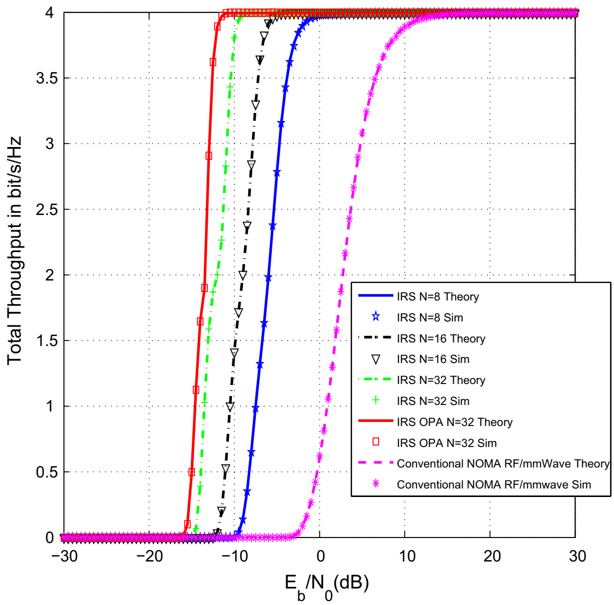

Fig. 5 Total throughput for 16QAM modulation: 2 users

Figure 7 depicts the total throughput for QPSK modulation when there are three users, i.e. $K = 3$. The fractions of allocated powers are ($C_1 = 0.2, C_2 = 0.3, C_3 = 0.5$) and ($D_1 = 0.2$, $D_2 = 0.3$, $D_3 = 0.5$). The proposed NOMA system using IRS offers 12, 14,

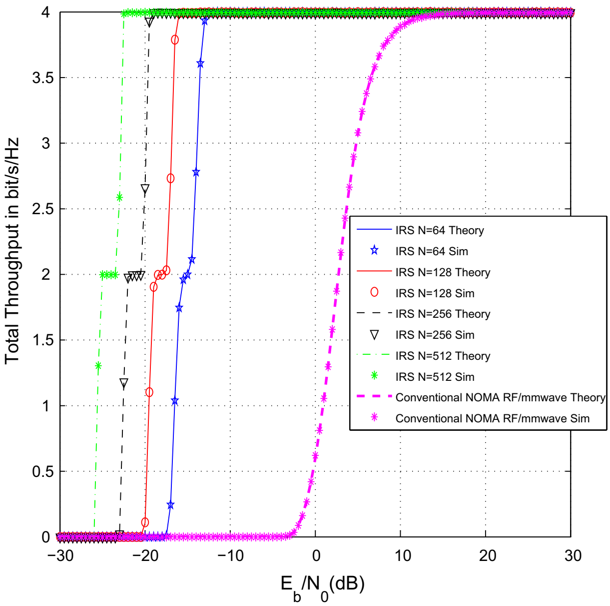

Fig. 6 Total throughput for 16QAM modulation: $N = 64, 128, 256, 512$

16 dB with respect to conventional NOMA system without IRS for a number of reflectors $N = N_1 = N_2 = N_3 = 8, 16, 32$. IRS with OPA (45) and $N = N_1 = N_2 = N_3 = 32$ reflectors offers 19 dB gain with respect to conventional NOMA using millimeter wave communication without IRS.

The required E_b/N_0 in dB to reach a total throughput of 2.5 bit/s/Hz is provided in Table 2 for different values of N. We used the results of Fig. 7 with three NOMA users and QPSK modulation.

6 Conclusions and Perspectives

In this paper, we used intelligent Reflecting Surfaces (IRS) to enhance the throughput of NOMA systems using millimeter wave communications. The source sends a combination of symbols to K users. The received signal at the relay node is affected with P interferers. The results are valid for any number of interferers at the relay and users. The relay node uses SIC to detect the symbols of all K NOMA users. Then, the relay node sends a combination of K detected symbols. The transmitted signal by relay node is reflected by different sets of reflectors dedicated to K users. The reflected signals by a set of IRS reflectors have the same phase at each user. The proposed NOMA

Table 1 Required E_b/N_0 in dB to reach a total throughput of 3.5 bit/s/Hz: two users and 16QAM modulation

N	512	256	128	64	32 OPA	32	16	8	No IRS
E_b/N_0	− 22.7	− 19.7	− 16.6	− 13.6	− 12.5	− 10.4	− 7.2	− 3.8	6.5

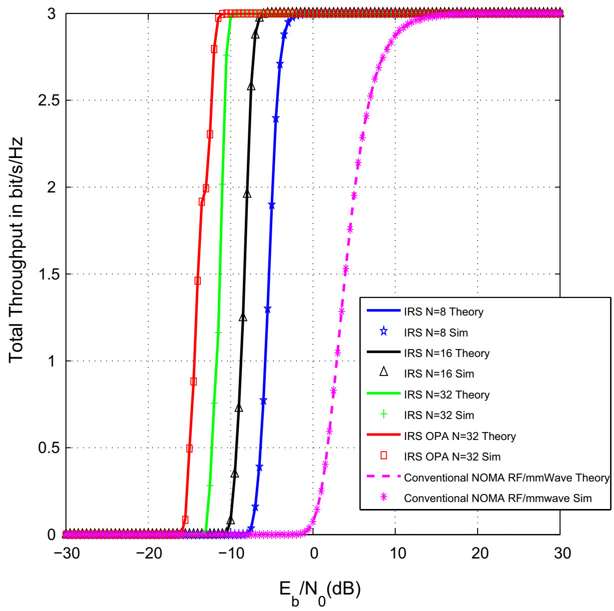

Fig. 7 Total throughput for QPSK modulation with optimal power allocation: 3 users

Table 2 Required E_b/N_0 in dB to reach a total throughput of 2.5 bit/s/Hz: three users and QPSK modulation

N	32 OPA	32	16	8	No IRS
E_b/N_0	− 12.3	− 10.7	− 7.6	− 4.3	6.9

using IRS offers 10, 13, 16, 20, 24, 27 and 30 dB gain with respect to conventional NOMA using millimeter wave communications without IRS for a number of reflectors $N = 8, 16, 32, 64, 128, 256, 512$. We also suggested optimizing the powers dedicated to NOMA users at the source and relay node to enhance the total throughput. As a perspective, we can consider millimeter wave communications with multihop relaying and IRS.

Appendix A

Let $X = E_S|f|^2$ and $I = \sum_{q=1}^{P} I_q$. U is defined as $U = \frac{X}{I}$. X and I are independent Gamma r.v. with PDF [36]

$$f_{X,I}(x,y) = \frac{x^{M-1}y^{PM-1}e^{-\frac{x}{\beta}}e^{-\frac{y}{\alpha}}}{\Gamma(M)\Gamma(MP)\beta^M\alpha^{MP}} \tag{46}$$

Let $U = \frac{X}{I}$ and $W = X + I$, the determinant of Jacobian matrix is

$$|J| = \begin{vmatrix} \frac{\partial U}{\partial X} & \frac{\partial U}{\partial I} \\ \frac{\partial W}{\partial X} & \frac{\partial W}{\partial I} \end{vmatrix} = \begin{vmatrix} \frac{1}{I} & \frac{-X}{I^2} \\ 1 & 1 \end{vmatrix} = \frac{X+I}{I^2} = \frac{(1+U)^2}{W} \tag{47}$$

We can write $I = \frac{W}{1+U}$ and $X = \frac{UW}{1+U}$. We deduce the PDF of (U, W)

$$\begin{aligned} f_{U,W}(u,w) = \frac{f_{X,I}(x,y)}{|J|} &= \frac{w}{(1+u)^2}\left(\frac{w}{1+u}\right)^{PM-1}\left(\frac{wu}{1+u}\right)^{M-1} \\ &\times \frac{e^{-\frac{wu}{(1+u)\beta}} e^{-\frac{w}{(1+u)\alpha}}}{\Gamma(M)\Gamma(MP)\beta^M \alpha^{MP}} \end{aligned} \tag{48}$$

We can write

$$f_U(u) = \int_0^{+\infty} f_{U,W}(u,w)dw. \tag{49}$$

We have [34]

$$\int_0^{+\infty} e^{-Aw} w^B dw = \frac{\Gamma(B+1)}{A^{B+1}} \tag{50}$$

Equations (29–31) give

$$f_U(u) = \frac{\Gamma(M+PM)\alpha^M u^{M-1}}{\beta^M \Gamma(M)\Gamma(PM)}\left(1 + \frac{u\alpha}{\beta}\right)^{-PM-M} \tag{51}$$

Author's contributions This article is the contribution of Prof. Raed Alhamad and Prof. Hatem Boujemaa.

Data availability Data and material are not available.

Declarations

Conflict of interest This publication was supported by Saudi Electronic University. The authors state that there is no conflict of interest for the current article.

References

1. Zöchmann, E., Groll, H., & Pratschner, S. (2019). A small-scale fading model for overtaking vehicles in a millimeter wave communication link. In: *2019 IEEE 20th international workshop on signal processing advances in wireless communications (SPAWC)*.
2. Jihao, L., Zhenfeng, Y., Yibing, L., Xiaohang, S., Ji, L., & Wei, Z. (2019). Research on millimeter wave phased array antenna for 5G communication. In: *2019 IEEE 2nd international conference on electronic information and communication technology (ICEICT)*.
3. Tsai, C.-H., Pepe, F., Mangraviti, G., Zong, Z., Craninckx, J., & Wambacq, P. (2019). A 22.5–27.7-GHz fast-lock bang-bang digital PLL in 28-nm CMOS for millimeter-wave communication with 220-fs RMS jitter. *IEEE Solid-State Circuits Letters, 2*(9), 232–239.
4. Pan, P., Zi, Z., Cai, J., & Feng, J. (2019). Millimeter wave vacuum electronic amplifiers for high data rate communication. In: *2019 44th international conference on infrared, millimeter, and terahertz waves (IRMMW-THz)*.

5. Kaur, J., & Singh, M. L. (2019). User assisted cooperative relaying in beamspace massive MIMO NOMA based systems for millimeter wave communications. *China Communications, 16*(6), 103–113.
6. Fukatsu, R., & Sakaguchi, K. (2019). Millimeter-wave V2V communications with cooperative perception for automated driving. In: *2019 IEEE 89th vehicular technology conference (VTC2019-Spring)*.
7. Zhang, J., Huang, Y., Xiao, M., Wang, J., & Yang, L. (2018). Energy-efficient cooperative hybrid precoding for millimeter-wave communication networks. In: *2018 IEEE global communications conference (GLOBECOM)*.
8. Zhang, J., Huang, Y., Zhang, C., He, S., Xiao, M., & Yang, L. (2017). Cooperative multi-subarray beam training in millimeter wave communication systems. In: *GLOBECOM 2017–2017 IEEE global communications conference*.
9. Kaur, J., & Singh, M. L. (2019). User assisted cooperative relaying in beamspace massive MIMO NOMA based systems for millimeter wave communications. *China Communications, 16*(6), 103–113.
10. Zhu, R., Wang, Y. E., Xu, Q., Liu, Y., & Li, Y. D. (2018). Millimeter-wave to microwave MIMO relays (M4R) for 5G building penetration communications. In: *IEEE radio and wireless symposium (RWS)*.
11. Basar, E., Di Renzo, M., De Rosny, J., Debbah, M., Alouini, M.-S., & Zhang, R. (2019). Wireless communications through Reconfigurable intelligent surfaces. *IEEE Access, 7*.
12. Zhang, H., Di, B., Song, L., & Han, Z. (2020). Reconfigurable intelligent surfaces assisted communications with limited phase shifts: How many phase shifts are enough? *IEEE Transactions on Vehicular Technology, 69*(4), 4498–4502.
13. Di Renzo, M. (2019). 6G Wireless: Wireless networks empowered by Reconfigurable intelligent surfaces. In: *2019 25th Asia-Pacific conference on communications (APCC)*.
14. Basar, E. (2020). Reconfigurable intelligent surface-based index modulation: A new beyond MIMO paradigm for 6G. *IEEE Transactions on Communications, Early Access Article*.
15. Wu, Q., & Zhang, R. (2020). Towards smart and reconfigurable environment: Intelligent reflecting surface aided wireless network. *IEEE Communications Magazine, 58*(1), 106–112.
16. Huang, C., Zappone, A., Alexandropoulos, G. C., Debbah, M., & Yuen, C. (2019). Reconfigurable intelligent surfaces for energy efficiency in wireless communication. *IEEE Transactions on Wireless Communications, 18*(8), 4157–4170.
17. Alexandropoulos, G. C. & Vlachos, E. (2020). A hardware architecture for reconfigurable intelligent surfaces with minimal active elements for explicit channel estimation. In: *ICASSP 2020–2020 IEEE international conference on acoustics, speech and signal processing (ICASSP)*.
18. Guo, H., Liang, Y.-C., Chen, J., & Larsson, E. G. (2020). Weighted sum-rate maximization for reconfigurable intelligent surface aided Wireless networks. *IEEE Transactions on Wireless Communications, Early Access Article*.
19. Thirumavalavan, V. C., & Jayaraman, T. S. (2020). BER analysis of reconfigurable intelligent surface assisted downlink power domain NOMA system. In: *2020 international conference on communication systems and networks (COMSNETS)*.
20. Chandan, P., Li, A., Song, L., Vucetic, B., & Li, Y. (2020). Hybrid precoding design for reconfigurable intelligent surface aided mmWave communication systems. *IEEE Wireless Communications Letters, Early Access Article*.
21. Ying, K., Gao, Z., Lyu, S., Wu, Y., Wang, H., & Alouini, M.-S. (2020). GMD-based hybrid beamforming for large reconfigurable intelligent surface assisted millimeter-wave massive MIMO. *IEEE Access, 8*, 19530–19539.
22. Di, B., Zhang, H., Li, L., Song, L., Li, Y., & Han, Z. (2020). Practical hybrid beamforming with finite-resolution phase shifters for reconfigurable intelligent surface based multi-user communications. *IEEE Transactions on Vehicular Technology, 69*(4), 4565–4570.
23. Nadeem, Q.-U.-A., Kammoun, A., Chaaban, A., Debbah, M., & Alouini, M.-S. (2020). Asymptotic max–min SINR analysis of reconfigurable intelligent surface assisted MISO systems. *IEEE Transactions on Wireless Communications, Early Access Article*.
24. Zhao, W., Wang, G., Atapattu, S., Tsiftsis, T. A., & Tellambura, C. (2020). Is backscatter link stronger than direct link in reconfigurable intelligent surface-assisted system. *IEEE Communications Letters, Early Access Article*.
25. Dai, L., Wang, B., Wang, M., Yang, X., Tan, J., Bi, S., Xu, S., Yang, F., Chen, Z., Di Renzo, M., Chae, C.-B., & Hanzo, L. (2020). Reconfigurable intelligent surface-based wireless communications: Antenna design, prototyping, and experimental results. *IEEE Access, 8*, 45913–45923.
26. Li, J., Li, X., Ye, N., & Wang, A. (2019). Performance evaluation of MIMO-NOMA in millimeter wave communication for broadcast services. *2019 IEEE international symposium on broadband multimedia systems and broadcasting (BMSB)*, Jeju-si, South Korea, 5–7 June 2019.

27. Azzahra, M. A., & Iskandar. (2019). NOMA signal transmission over millimeter-wave frequency for backbone network in HAPS with MIMO antenna. In: *2019 IEEE 13th international conference on telecommunication systems, services, and applications (TSSA)*.
28. Jaipreet, K., & Singh, M. L. (2019). User assisted cooperative relaying in beamspace massive MIMO NOMA based systems for millimeter wave communications. *China Communications, 16*(6), 103–113.
29. Guo, L., Cong, S., & Su, C. (2020). On coverage probability of uplink NOMA in millimeter wave cellular networks. *2020 9th Asia-Pacific conference on antennas and propagation (APCAP), 4–7*.
30. Luo, Z., Zhao, L., Tonghui, L., Liu, H., & Zhang, R. (2021). Robust hybrid precoding/combining designs for full-duplex millimeter wave relay systems. *IEEE Transactions on Vehicular Technology: Early Access Articles*.
31. Ma, K., He, D., Sun, H., Wang, Z., & Chen, S. (2021). Deep learning assisted calibrated beam training for millimeter-wave communication systems. *IEEE Transactions on Communications, Early Access Articles*.
32. Wen, L., Zhiqiang, Y., Zhu, L., Zhou, J. (2021). High-gain dual-band resonant cavity antenna for 5G millimeter wave communications. *IEEE Antennas and Wireless Propagation Letters, Early Access Articles*.
33. Ghasemi, A., & Sousa, E. S. (2007). Fundamental limits of spectrum-sharing in fading environments. *IEEE Transactions on Wireless Communications, 6*(2), 649–658.
34. Gradshteyn, I. S., & Ryzhik, I. M. (1994). *Table of integrals, series and products* (5th ed.). CA, Academic: San Diego.
35. Xi, Y., Burr, A., Wei, J. B., & Grace, D. (2011). A general upper bound to evaluate packet error rate over quasi-static fading channels. *IEEE Transactions on Wireless Communications, 10*(5), 1373–1377.
36. Proakis, J. (2007). *Digital communications* (5th.). Mac Graw-Hill.

Raed Alhamad received his B.S. at Information Systems Technology and Minor of Network Security from Southern Illinois University(SIUC), Carbondale, Illinois, in 2009, And the M.Eng. and Ph.D. degrees from Stevens Institute of Technology at Networked Information Systems in 2011 and Electrical Engineering in 2015, respectively. Also, In 2016 he got Edward Peskin Award. Dr. Alhamad has been a faculty member at Saudi Electronic University since 2014. He is an associate professor. His research interests include wireless communications, networking, and cyber security.

Hatem Boujemaa was born in Tunis, Tunisia. He received the Engineer's Diploma from "Ecole Polytechnique de Tunis", in 1997, the MSC in digital communications from "Telecom Paris Tech", in 1998 and the Ph.D. degree in electronics and communications from the same university in 2001. From October 1998 to September 2001, he prepared his Ph.D. degree at France Telecom R&D, Issy-les-Moulineaux, France. During this period, he participated in the RNRT project AUBE. From October 2001 to January 2002, he joined "Ecole Supérieure d'Electricité", Gif-sur- Yvette, France, and worked on mobile localization for RNRT project LUTECE. In February 2002, he joined SUPCOM where he is a Professor. His research activities are in the field of digital communications, DS-CDMA, OFDM and MC-CDMA systems, HARQ protocols, Cooperative Communications, Cognitive radio networks, spectrum sensing, Scheduling, Synchronization, Network planning, Information Theory, Equalization and Antenna Processing.